From Poor-Active to High-Performance *via* Heteroleptic Tetrahedra Engineering: Rational Design of Non-π-Conjugated Hybrids for Phase-Matchable Ultraviolet Nonlinear Optics

Ming-Chang Wang,[a] Mo-Fan Zhuo,[a] Zhi Lin,[a] Jia-Jia Li,[a] Miao-Bing Xu,[a] Yun-Xia Hu,[a] Jia-Min Lian,[a] Ke-Zhao Du[a,b]* and Jin Chen[a,b]*

a Fujian Provincial Key Laboratory of Advanced Materials Oriented Chemical Engineering, Collage of Chemistry and Material Science, Fujian Normal University, Fuzhou 350007, China

b State Key Laboratory of Structural Chemistry, Fujian Institute of Research on the Structure of Matter, Chinese Academy of Sciences, Fuzhou, 350002, P. R. China

Table S1. Crystallographic data.

Compound	**$(H_2DABCO)CdI_4$**	**$(PIP)\cdot CdI_3(HDABCO)$**
empirical formula	$C_6H_{14}CdI_4N_2$	$C_{10}H_{23}CdI_3N_4$
formula weight	734.19	692.42
crystal system	orthorhombic	monoclinic
space group	$P2_12_12_1$	Cc
T (K)	293(2)	295.11(10)
a (Å)	8.9818(2)	7.7434(9)
b (Å)	12.6343(2)	24.318(3)
c (Å)	14.5462(3)	10.2941(14)
β / °	90	92.722(12)
V (Å^3)	1650.68(6)	1936.2(4)
Z	4	4
ρ_{calc} (g/cm^3)	2.954	2.375
μ (mm^{-1})	69.109	5.904
goodness of fit on F^2	1.061	1.053
R_1, wR_2 [$I > 2\sigma(I)$][a]	0.0681, 0.1887	0.0589, 0.1426
R_1, wR_2 [all data][a]	0.0745, 0.1953	0.0642, 0.1505
Flack factor	-0.11(10)	-0.02(4)

[a] $R_1 = \sum||F_o| - |F_c||/\sum|F_o|$, and $wR_2 = \{\sum w[(F_o)^2 - (F_c)^2]^2/\sum w[(F_o)^2]^2\}^{1/2}$

Table S2. Fractional Atomic Coordinates (× 10^4) and Equivalent Isotropic Displacement Parameters (Å^2 × 10^3) for **$(H_2DABCO)CdI_4$** and **$(PIP)\cdot CdI_3(HDABCO)$**.

$(H_2DABCO)CdI_4$

Atom	x	y	z	U(eq)
I1	9960.1(13)	4020.8(10)	4533.5(8)	48.8(4)
I2	4928.2(15)	4302.1(14)	4534.3(11)	64.5(5)
I3	8053(2)	7250.5(14)	4160.4(12)	74.8(6)
I4	7445.5(17)	5362.2(13)	6918.5(9)	60.8(4)
Cd1	7544.8(16)	5327.5(12)	4990.8(10)	53.2(4)
N1	8809(18)	953(16)	2263(11)	51(4)
N2	6370(20)	1378(19)	3008(19)	78(7)
C1	7710(30)	1380(20)	1540(17)	67(6)
C2	6280(40)	1610(30)	1970(20)	83(9)
C3	9040(20)	1750(20)	2977(17)	56(5)
C4	7590(30)	2000(20)	3442(15)	61(5)
C5	8160(30)	-35(19)	2678(19)	66(7)
C6	6710(30)	208(18)	3100(20)	76(8)

(PIP)·CdI_3(HDABCO)

Atom	x	y	z	U(eq)
I1	6160.1(18)	1217.4(6)	7229.8(15)	58.1(4)
I2	6617.9(18)	1024.7(6)	2751.7(15)	61.5(4)
I3	1573.0(14)	1591.7(5)	4290.5(12)	51.8(4)
Cd1	5109.1(16)	1541.8(4)	4754.5(13)	42.4(4)
N1	6480(20)	3500(5)	4548(15)	43(3)
N2	5762(18)	2464(5)	4683(13)	35(3)
N3	6620(20)	4614(6)	3929(15)	47(4)
N4	6610(20)	5278(6)	6240(14)	45(4)
C1	7930(30)	3203(8)	5180(20)	52(5)
C2	7570(30)	2584(8)	5140(30)	65(6)
C3	4600(30)	2791(8)	5480(20)	57(5)
C4	4910(30)	3410(7)	5330(20)	47(4)
C5	6060(30)	3267(8)	3239(18)	48(4)
C6	5500(30)	2668(8)	3344(19)	57(5)
C7	8230(30)	4868(8)	4470(20)	57(5)
C8	8120(30)	4944(9)	5940(20)	58(5)
C9	5020(30)	5017(9)	5700(20)	56(5)
C10	5080(30)	4922(8)	4250(20)	57(5)

Table S3. Bond Lengths for **$(H_2DABCO)CdI_4$** and **(PIP)·CdI_3(HDABCO)**.

$(H_2DABCO)CdI_4$

Atom	Atom	Length/Å	Atom	Atom	Length/Å
I1	Cd1	2.81(19)	N2	C2	1.54(4)
I2	Cd1	2.77(2)	N2	C4	1.50(3)
I3	Cd1	2.75(2)	N2	C6	1.51(4)
I4	Cd1	2.81(2)	C1	C2	1.47(4)
N1	C1	1.54(3)	C3	C4	1.50(3)
N1	C3	1.46(3)	C5	C6	1.48(3)
N1	C5	1.50(3)			

(PIP)·CdI_3(HDABCO)

Atom	Atom	Length/Å	Atom	Atom	Length/Å
I1	Cd1	2.75(2)	N3	C7	1.47(3)
I2	Cd1	2.73(19)	N3	C10	1.47(3)
I3	Cd1	2.76(17)	N4	C8	1.47(3)

Cd1	N2	2.30(13)	N4	C9	1.47(3)
N1	C1	1.46(3)	C1	C2	1.53(3)
N1	C4	1.51(2)	C3	C4	1.53(3)
N1	C5	1.48(2)	C5	C6	1.53(3)
N2	C2	1.48(2)	C7	C8	1.53(3)
N2	C3	1.48(2)	C9	C10	1.51(3)
N2	C6	1.47(2)			

Table S4. Bond Angles for **$(H_2DABCO)CdI_4$** and **$(PIP)\cdot CdI_3(HDABCO)$**.

$(H_2DABCO)CdI_4$

Atom	Atom	Atom	Angle/	Atom	Atom	Atom	Angle/
I2	Cd1	I1	108.94(7)	C4	N2	C2	110.00(2)
I2	Cd1	I4	102.73(6)	C4	N2	C6	109.00(2)
I3	Cd1	I1	106.69(7)	C6	N2	C2	107.00(2)
I3	Cd1	I2	116.70(8)	C2	C1	N1	110.00(2)
I3	Cd1	I4	115.48(8)	C1	C2	N2	109.00(2)
I4	Cd1	I1	105.70(6)	N1	C3	C4	110.20(16)
C3	N1	C1	109.70(18)	N2	C4	C3	109.50(17)
C3	N1	C5	110.00(17)	C6	C5	N1	109.60(18)
C5	N1	C1	109.00(2)	C5	C6	N2	110.10(18)

$(PIP)\cdot CdI_3(HDABCO)$

Atom	Atom	Atom	Angle/	Atom	Atom	Atom	Angle/
I1	Cd1	I3	114.84(6)	C6	N2	C3	106.20(16)
I2	Cd1	I1	116.71(7)	C10	N3	C7	112.60(15)
I2	Cd1	I3	110.29(6)	C8	N4	C9	109.90(15)
N2	Cd1	I1	104.70(3)	N1	C1	C2	110.10(15)
N2	Cd1	I2	108.80(3)	N2	C2	C1	111.60(16)
N2	Cd1	I3	99.80(4)	N2	C3	C4	111.70(14)
C1	N1	C4	108.40(15)	N1	C4	C3	109.30(14)
C1	N1	C5	110.20(16)	N1	C5	C6	110.50(15)
C5	N1	C4	106.20(16)	N2	C6	C5	111.20(16)
C2	N2	Cd1	112.80(11)	N3	C7	C8	109.90(17)
C3	N2	Cd1	111.50(10)	N4	C8	C7	110.80(19)
C3	N2	C2	107.80(17)	N4	C9	C10	112.10(18)
C6	N2	Cd1	109.70(10)	N3	C10	C9	111.40(18)
C6	N2	C2	108.50(16)				

[1]+X,+Y,1+Z; [2]1-X,1-Y,1-Z; [3]1-X,1-Y,-Z; [4]+X,+Y,-1+Z; [5]+X,+Y,-Z

Table S5. The assignments of the infrared absorption peaks for **$(H_2DABCO)CdI_4$** and **$(PIP)\cdot CdI_3(HDABCO)$**.

Assignment (cm^{-1})	**$(H_2DABCO)CdI_4$**	**$(PIP)\cdot CdI_3(HDABCO)$**
$-CH_2-$	1466	1445
C-H	3005	2944, 2876
N-H	3072	3225
C-C	1048	1053
C-N	1381	1344, 1369
Cd-N	\	490

Table S6. Hydrogen Bonds for **$(PIP)\cdot CdI_3(HDABCO)$**.

D	H	A	d(D-H)/Å	d(H-A)/Å	d(D-A)/Å	D-H-A/°
N1	H1	N3	0.98	1.85	2.79(2)	159.6
N4	H4D	N3[1]	0.89	1.89	2.78(2)	175.5

[1]+X,1-Y,1/2+Z

Table S7. Calculated dipole moment for CdI_4, $CdNI_3$ tetrahedron and net dipole moment for a unit cell in **$(H_2DABCO)CdI_4$** and **$(PIP)\cdot CdI_3(HDABCO)$**.

$(H_2DABCO)CdI_4$ (Z = 4)

Polar unit	Dipole moment (D=Debyes)			
	x-component	y-component	z-component	Total magnitude
$Cd(1)I_4$	0.918	-2.641	1.343	3.102
$Cd(2)I_4$	-0.918	2.641	1.343	3.102
$Cd(3)I_4$	0.918	2.641	-1.343	3.102
$Cd(4)I_4$	-0.918	-2.641	-1.343	3.102
Net dipole moment (a unit cell)	5.26×10^{-8}	6.13×10^{-8}	1.40×10^{-6}	6.13×10^{-5}
Dipole moment per unit volume (Debyes / $Å^3$)	3.72×10^{-8}			

$(PIP)\cdot CdI_3(HDABCO)$ (Z = 4)

Polar unit	Dipole moment (D=Debyes)			
	x-component	y-component	z-component	Total magnitude
$Cd(1)NI_3$	-3.175	5.945	-0.347	6.748
$Cd(2)NI_3$	-3.175	-5.945	-0.347	6.748

$Cd(3)NI_3$	-3.175	5.945	-0.347	6.748
$Cd(4)NI_3$	-3.175	5.945	-0.347	6.748
Net dipole moment (a unit cell)	-12.698	11.889	-1.387	17.451
Dipole moment per unit volume (Debyes/ $Å^3$)	9.01×10^{-3}			

Table S8. SHG response and bandgap of representative d^{10}-TM and SCALP cation based NLO OIMHs.

Compound	Metal cation	Organic group	Band gap (eV)	SHG response (× KDP)	Ref.
$(H_2DABCO)CdI_4$	d^{10}-TM cation	non-π-conjugated group	3.84	0.3	This work
$(PIP)\cdot CdI_3(HDABCO)$	d^{10}-TM cation	non-π-conjugated group	4.05	2.1	
$H_{12}C_4N_2CdI_4$	d^{10}-TM cation	non-π-conjugated group	3.86	0.5	29 [a]
$H_{11}C_4N_2CdI_3$	d^{10}-TM cation	non-π-conjugated group	4.10	6.0	29 [a]
$(C_5H_{14}NO)CdCl_3$	d^{10}-TM cation	non-π-conjugated group	4.41	0.40	51 [a]
$[(CH_3)_3NCH_2Cl]CdCl_3$	d^{10}-TM cation	non-π-conjugated group	5.24	0.73	52 [a]
$(L\text{-}Hpro)_2Cd_5Cl_{12}$	d^{10}-TM cation	π-conjugated group	5.42	0.25	1
(L-Hpro)(L-pro)$CdCl_3$	d^{10}-TM cation	π-conjugated group	5.61	0.69	1
$(C_4H_{10}NO)_2Cd_2Cl_6$	d^{10}-TM cation	π-conjugated group	5.45	0.73	2
$(C_{13}N_3H_{14})_2CdBr_4$	d^{10}-TM cation	π-conjugated group	3.98	0.98	53 [a]
$L\text{-}C_{12}H_{20}N_6O_4Cd_2Cl_5$	d^{10}-TM cation	π-conjugated group	5.01	0.25	3
$D\text{-}C_{12}H_{20}N_6O_4Cd_2Cl_5$	d^{10}-TM cation	π-conjugated group	4.97	0.30	3
$ZnBr(C_6H_{3.5}FNO_2)_2$	d^{10}-TM cation	π-conjugated	4.20	1.70	55 [a]

		group			
$(C_4H_{11}N_2)ZnCl_3$	d^{10}-TM cation	non-π-conjugated group	> 6.20	0.80	30 [a]
$(C_4H_{11}N_2)ZnBr_3$	d^{10}-TM cation	non-π-conjugated group	5.53	2.50	30 [a]
$(C_4H_{11}N_2)ZnI_3$	d^{10}-TM cation	non-π-conjugated group	4.52	2.10	30 [a]
$(C_5H_6N)SbF_2SO_4$	SCALP cation	π-conjugated group	4.28	1.60	19 [a]
$(C_4H_{10}NO)PbCl_3$	SCALP cation	π-conjugated group	3.55	0.70	4
$(C_4H_{10}NO)PbBr_3$	SCALP cation	π-conjugated group	3.60	0.80	4
$[C_8N_2H_{22}][PbI_4]$	SCALP cation	π-conjugated group	2.36	2.61	5
$(C_{10}H_{11}N_3)PbCl_4$	SCALP cation	π-conjugated group	3.35	3.80	6
$(C_{10}H_{11}N_3)PbBr_4$	SCALP cation	π-conjugated group	2.95	5.00	6
(R/S)-$[(C_8H_{10}NO_3)_2]Sn(IV)F_6$	SCALP cation	π-conjugated group	4.21	0.46	7
(R/S)-$[C_8H_{10}NO_3]Sn(II)F_3$	SCALP cation	π-conjugated group	4.18	0.85	7
$(2\text{-AMP})_2BiCl_7 \cdot H_2O$	SCALP cation	π-conjugated group	3.28	0.25	8
$(2\text{-AMP})_2BiBr_7 \cdot H_2O$	SCALP cation	π-conjugated group	2.84	0.32	8
$[C_8N_2H_{22}]_{1.5}[Bi_2I_9]$	SCALP cation	π-conjugated group	1.98	1.29	54 [a]
$(C_6H_5(CH_2)_4NH_3)_4BiBr_7 \cdot H_2O$	SCALP cation	π-conjugated group	3.52	0.40	50 [a]

[a] the references in the table refer to those in the main text.

Table S9. The dipole moment per unit volume (metal centered polyhedra) and SHG response for several d^{10}-TM cations based OIMHs.

Compound	Total magnitude	Volume/Å^3	Dipole moment per unit volume (Debyes/ Å^3)	SHG response (× KDP)	Ref.

$(H_2DABCO)CdI_4$	6.13×10^{-5}	1650.68	3.72×10^{-8}	0.3	This
(PIP)·CdI_3(HDABCO)	17.45	1936.20	9.01×10^{-3}	2.1	work
$H_{12}C_4N_2CdI_4$	0.02	1442.37	1.14×10^{-5}	0.5	29 [a]
$H_{11}C_4N_2CdI_3$	17.09	1206.88	1.42×10^{-2}	6.0	29 [a]
$(C_{13}N_3H_{14})_2CdBr_4$	21.46	3075.60	6.98×10^{-3}	0.98	53 [a]
$[(CH_3)_3NCH_2Cl]CdCl_3$	0.70	1012.84	6.87×10^{-4}	0.73	52 [a]
D-$C_{12}H_{20}N_6O_4Cd_2Cl_5$	1.19	585.96	2.03×10^{-3}	0.2	3
L-$C_{12}H_{20}N_6O_4Cd_2Cl_5$	1.20	584.34	2.05×10^{-3}	0.2	3
$(C_5H_{14}NO)CdCl_3$	0.10	1076.68	9.61×10^{-5}	0.4	51 [a]
$(C_4H_{11}N_2)ZnCl_3$	2.06	229.271	9.01×10^{-3}	0.8	30 [a]
(C4H11N2)ZnBr3	5.11	255.81	2.00×10^{-2}	2.5	30 [a]
(C4H11N2)ZnI3	42.80	2352.34	1.82×10^{-2}	2.1	30 [a]
$(C_3N_6H_7)(C_3N_6H_6)HgCl_3$	1.22	764.72	1.60×10^{-3}	5.0	9
$(C_{13}N_3H_{14})_2ZnBr_4$	20.47	3031.7	6.75×10^{-3}	1.12	53 [a]

[a] the references in the table refer to those in the main text.

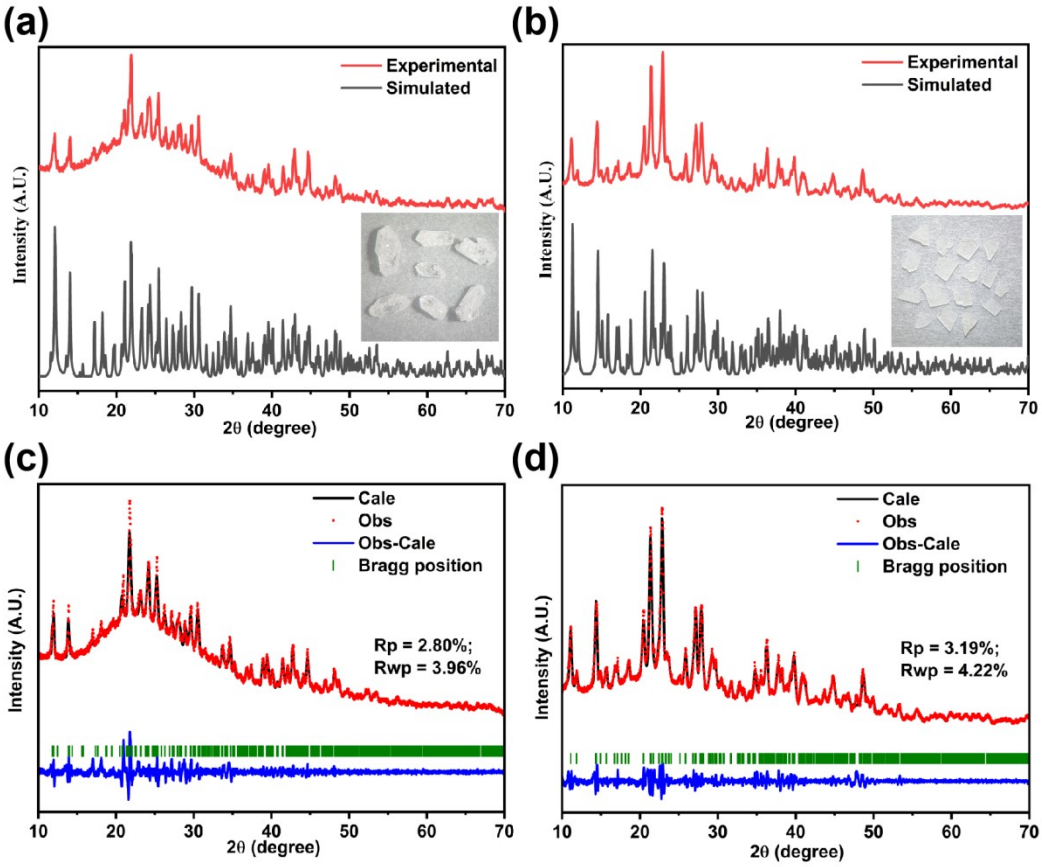

Figure S1. Simulated and measured powder X-ray diffraction patterns for **$(H_2DABCO)CdI_4$** (a) and **$(PIP)\cdot CdI_3(HDABCO)$** (b); refined PXRD data for **$(H_2DABCO)CdI_4$** (c) and **$(PIP)\cdot CdI_3(HDABCO)$** (d). The inside pictures are the corresponding crystals photos.

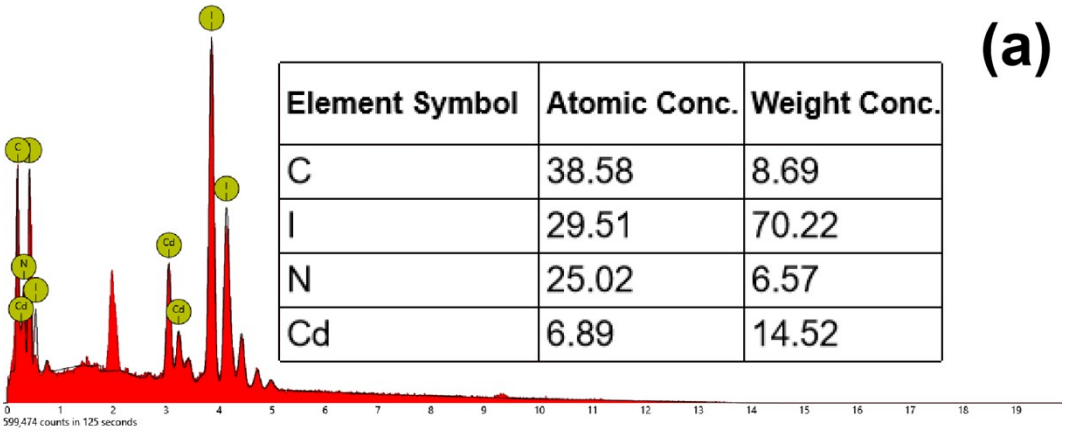

Element Symbol	Atomic Conc.	Weight Conc.
C	38.58	8.69
I	29.51	70.22
N	25.02	6.57
Cd	6.89	14.52

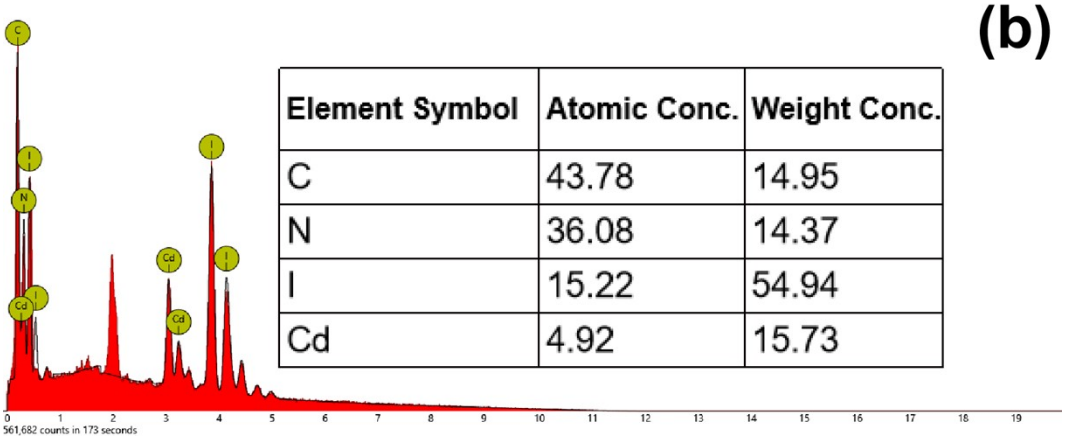

Element Symbol	Atomic Conc.	Weight Conc.
C	43.78	14.95
N	36.08	14.37
I	15.22	54.94
Cd	4.92	15.73

Figure S2. EDS for $(H_2DABCO)CdI_4$ (a) and $(PIP)\cdot CdI_3(HDABCO)$ (b).

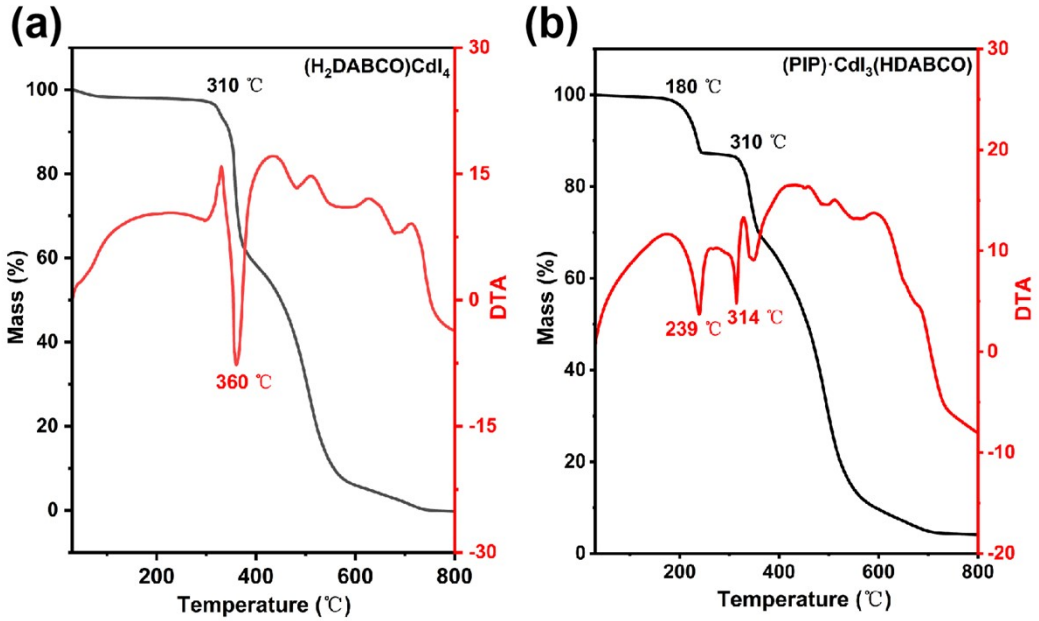

Figure S3. TG-DTA curves for **$(H_2DABCO)CdI_4$** (a) and **$(PIP)\cdot CdI_3(HDABCO)$** (b).

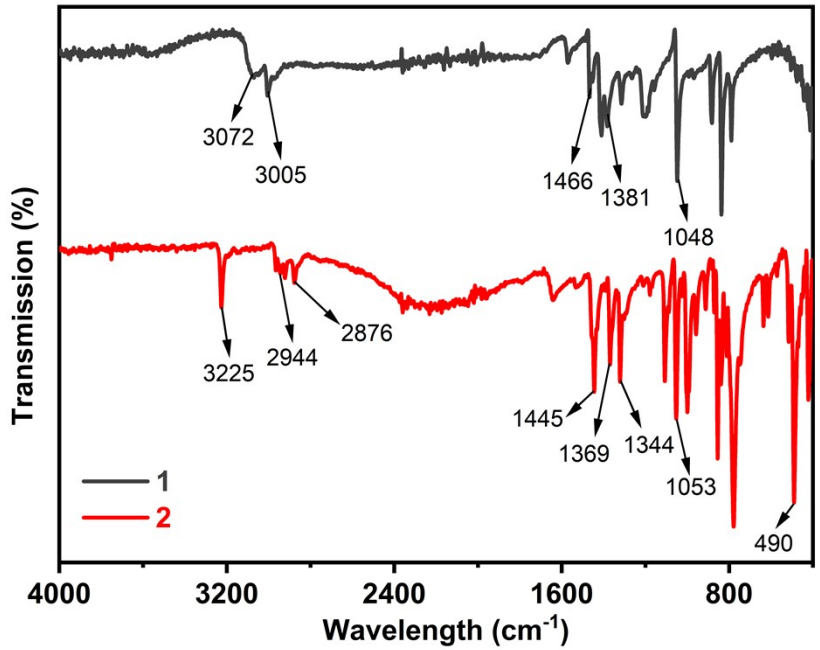

Figure S4. IR spectra for title compounds (curve 1 for **$(H_2DABCO)CdI_4$** and 2 for **$(PIP)\cdot CdI_3(HDABCO)$**, respectively).

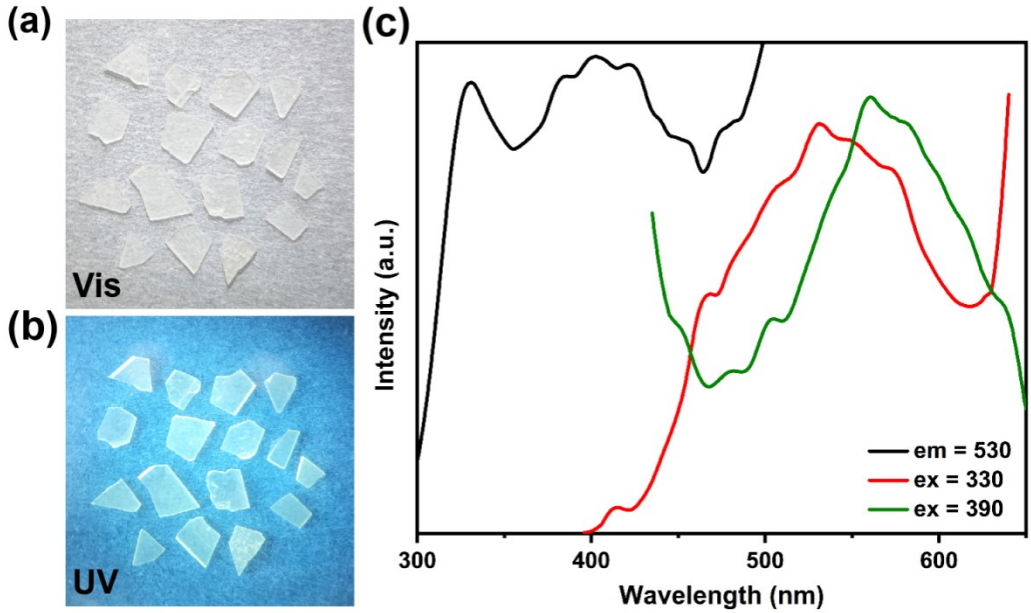

Figure S5. Crystals under visible (a) and ultraviolet light (b). PL and PLE spectra of **$(PIP)\cdot CdI_3(HDABCO)$** (c).

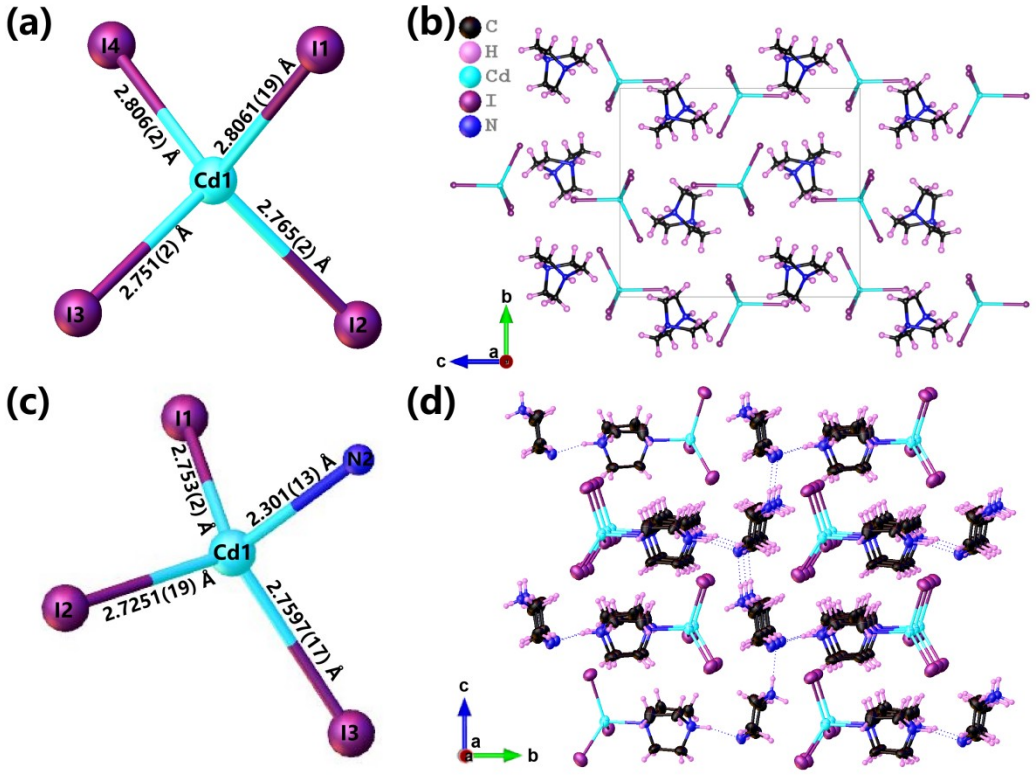

Figure S6. the bond lengths of the two types of tetrahedra, CdI_4 (a) and $CdNI_3$ (c); the quasi-two-dimensional (quasi-2D) $[H_2DABCOCdI_4]$ layer in **$(H_2DABCO)CdI_4$** (b), the hydrogen bond in compound **$(PIP)\cdot CdI_3(HDABCO)$** (d).

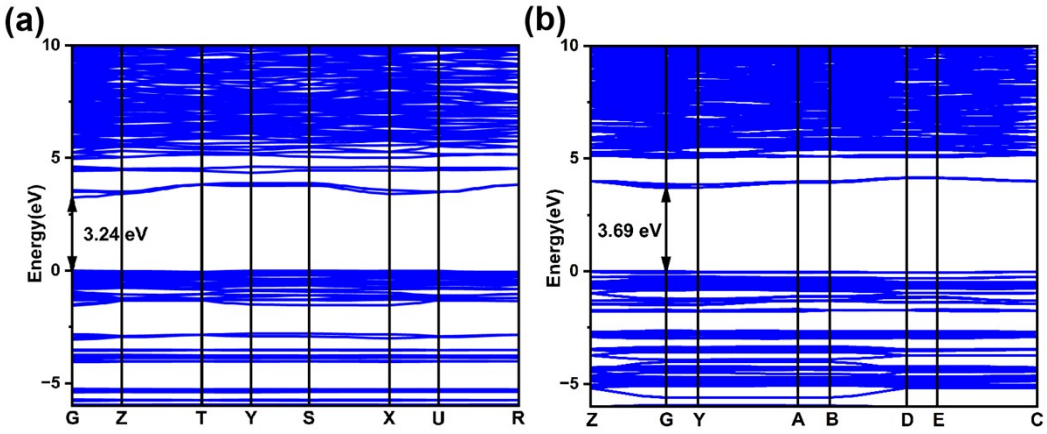

Figure S7. The calculated band structures of **$(H_2DABCO)CdI_4$** (a) and **$(PIP)\cdot CdI_3(HDABCO)$** (b).

References

1. J. Cheng, Y. Deng, X. Dong, J. Li, L. Huang, H. Zeng, G. Zou and Z. Lin, Homochiral Hybrid Organic‐Inorganic Cadmium Chlorides Directed by Enantiopure Amino Acids, *Inorg. Chem.*, 2022, **61**, 11032-11035.
2. D. Sun, D. Wang, Y. Dang, S. Zhang, H. Chen, R. Hou, K. Wu and C. Shen, Organic‐Inorganic Hybrid Noncentrosymmetric (Morpholinium)$_2$Cd$_2$Cl$_6$ Single Crystals: Synthesis, Nonlinear Optical Properties, and Stability, *Inorg. Chem.*, 2022, **61**, 8076-8082.
3. W. Seo and K. M. Ok, Novel noncentrosymmetric polar coordination compounds derived from chiral histidine ligands, *Inorg. Chem. Front.*, 2021, **8**, 4536-4543.
4. C. Shen, D. Sun, Y. Dang, K. Wu, T. Xu, R. Hou, H. Chen, J. Wang and D. Wang, ($C_4H_{10}NO$)PbX_3 (X = Cl, Br): Design of Two Lead Halide Perovskite Crystals with Moderate Nonlinear Optical Properties, *Inorg. Chem.*, 2022, **61**, 16936-16943.
5. Z. Chen, G. Zhang, J. Wen, Z. Liu, S. Chen, J. Hou and Y. Fang, Switchable Photovoltaic Effect and Robust Nonlinear Optical Response in a High-Temperature Molecular Ferroelectric [$C_8N_2H_{22}$][PbI_4], *Inorg. Chem.*, 2024, **63**, 21275-21282.
6. L.-L. Zhang, Q. Ding, P. Wang, Y. Zhang, Q.-Y. Liu, Y.-L. Wang and J. Luo, Achieving strong second harmonic generation effects induced via dimensional increase of PbX_6 octahedra and halogen substitutes in ($C_{10}H_{11}N_3$)PbX_4 (X = Cl or Br), *Inorg. Chem. Front.*, 2024, **11**, 3618-3625.
7. A. Jung, Y. Li and K. M. Ok, Chiral amino acid-templated tin fluorides tailoring nonlinear optical properties, birefringence, and photoluminescence, *Dalton Trans.*, 2024, **53**, 105-114.
8. D. Sun, D. Wang, H. Chen, R. Hou, Y. Dang, K. Wu, J. Wang and C. Shen, New Low-Dimensional Lead-Free Perovskite (2-AMP)2BiX_7 • H_2O (X = Cl, Br) Crystals: Synthesis, Stability, and Nonlinear Optical Properties, *Inorg. Chem.*, 2022, **61**, 15247-15255.
9. Z. Bai, J. Lee, H. Kim, C.-L. Hu and K. M. Ok, Unveiling the Superior Optical Properties of Novel Melamine-Based Nonlinear Optical Material with Strong Second-Harmonic Generation and Giant Optical Anisotropy, *Small*, 2023, **19**, 2301756.